International Journal of Thermophysics, Vol. 11, No. 1, 1990

Direct Observation of Critical Fluctuations in a Binary Mixture

D. Beysens,[2] P. Guenoun,[2] and F. Perrot[2]

Microscopic observations of concentration fluctuations in the range 1–500 μm have been performed in a number of binary fluids near their critical temperature (T_c). A heterodyne technique has been used. The temperature range ($T - T_c =$ 1–25 mK) is such that the sizes of the fluctuations are larger than or equal to the correlation length, measured usually as the inverse half-width of the structure factor of the fluctuations. Image analysis has given some information about the free energy of the system determined from the intensity distribution function. Also, the shape of the fluctuations can be studied. These are self-similar over more than three decades, with a fractal dimension of $D_f = 2.8$. This value is compared with a number of theoretical predictions.

KEY WORDS: concentration fluctuations; critical phenomena; fractal dimensionality; liquid mixtures; percolation.

1. INTRODUCTION

What is the interest in visually observing fluctuations near a continuous phase transition? The degree of knowledge of critical phenomena is such that it seems that nothing really new might come out from such a study. The behavior of fluids and fluid mixtures, which belong to the same universality class as the 3-D Ising model, has been much investigated and has led to a deep understanding of critical behavior [1]. We notice, however, that all experimental methods that have been used, including light-scattering techniques, enable only spatially averaged information to be obtained. The order parameter fluctuations are investigated through their correlation function $C(\vec{r})$ or equivalently through their structure factor $S(\vec{k})$ (here $\vec{r}$ is

[1] Paper presented at the Tenth Symposium on Thermophysical Properties, June 20–23, 1988, Gaithersburg, Maryland, U.S.A.

[2] Service de Physique du Solide et de Résonance Magnétique, CEA-CEN Saclay, 91191 Gif-sur-Yvette Cedex, France.

0195-928X/90/0100-0037$06.00/0

a space coordinate and $\vec{k}$ a wavevector). The typical length ξ (the so-called "correlation length") at which $S(k\xi)$ takes the value 1/2 can be used as a measurement of the approach of the critical point. Although the static statistical properties of critical fluctuations are well-known, as are, to a lesser extent, the corresponding dynamical properties, no valuable local investigation method is available. A pioneering attempt by Debye and Jacobsen [2] was performed in the late 1960s. They used a phase-contrast microscope to observe in direct space concentration fluctuations which develop near the critical point of a polymer–solvent system of polystyrene and cyclohexane. They immersed both the microscope and the sample in an air thermostat which was controlled to within ± 0.02 K; this thermal accuracy did not allow clear separation of the critical fluctuations from the onset of phase separation. No images were reported. No further developments were made after Debye's death. To our knowledge, no other attempts have been reported up to the present study.

Although the pedagogical interest of such observations is obvious, some limitations exist concerning the visualization technique. They are twofold: the image is by necessity a planar section (or a projection or both) of the bulk system, and the resolution is limited to typically 1 μm. The ultimate image resolution, or picture element (pixel) δr, will have to remain in a range $\delta r \gtrsim 1$ μm ($\simeq \xi$ at $T - T_c = 1$ mK).

It was therefore very surprising to us that we could actually detect well-defined fluctuations, in a temperature range $T - T_c < 25$ mK (or $\xi > 0.2$ μm) and whose typical length scale ranged up to the sample size. Another surprise came from the fractal-like shape of the fluctuations. These observations can, however, be related to some unusual aspects of critical-point phenomena.

We believe that such a local and direct observation of critical fluctuations should elucidate the modern view of critical phenomena. For instance, it becomes possible to study the statistics of such fluctuations, whose high degree of correlation would allow Wilson's effective free energy to be measured. The morphology of these fluctuations is striking, and the measure of a fractal exponent would provide new insight into the possible connection between thermal and percolation critical points, where the fluctuations are considered as domains percolating at T_c.

There are also a number of problems of current interest that could be studied. The 2, 4..., point correlation functions could be determined; the statics and dynamics of fluctuations under an external field (shear flow, thermal gradient, gravity, etc.) or at an interface solid–mixture or between the two phases below T_c could be followed. Dynamics related to a distribution of length scales (stretched exponential) could also be investigated [3].

2. EXPERIMENTAL

Binary mixtures have been used because they allow a close approach to T_c to be made without noticeable gravity effects. Thermal stabilization was of the order of ± 0.2 mK over a few hours and was provided by a water bath. Such a water thermostat suppresses the temperature gradients in the sample.

The experimental cell (Fig. 1) was 2 mm thick so that multiple scattering close to T_c does not blur the image. A high-quality photo lens (50- or 100-mm focal length; f, 1.0 or 1.8 aperture) has been used in order to have a large working distance. A magnified image of the bulk system is directly formed on the sensitive photocathode of a video camera (CCD or Newicon tube). The ultimate optical resolution (one pixel) corresponds to 1 μm in the sample. For this resolution the field of view is of order 250 μm.

The large aperture angle of the lens ($\simeq 90°$) ensures that the image is the projection of the bulk within a layer whose thickness is of the order of the resolution limit. The image is therefore simply a section of the bulk sample.

The cell was illuminated by a nearly parallel white light beam (Fig. 1), whose temporal coherence length is of the order of 1 μm. The image of the refractive index fluctuations $\delta n(\vec{r}, t)$ can be interpreted as being formed by the interference of the transmitted beam (E_T) with the light scattered by the above fluctuations (E_S). This corresponds to a "heterodyne" arrangement. The use of more coherent light (laser) is not useful, On the contrary, it adds numerous interference patterns which blur the final image.

The fact that $\langle \delta n^2 \rangle$ increases near T_c makes E_s increase, so that the contrast C of the above fluctuations becomes larger. This contrast

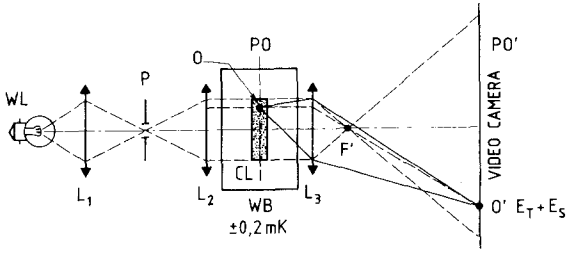

Fig. 1. Schematic of the setup. CL, sample cell containing the binary fluid; WB, water bath for temperature control; WL, white lamp source; L_1 and L_2, lenses; L_3, high-quality, large aperture, objective; F', focus of L_3; P, pinhole; PO, plane of the object, whose image is in PO'; O, point object in PO, whose image is at O'. (—) Path of the direct light, with transmitted field E_T; (—) path of the scattered light, with scattered field E_S.

decreases with $T-T_c$. The intensity detected on the video camera plane (x, y) can thus be written as

$$i(x, y) \propto |E_0|^2 + E_0 E_S(x, y) \propto 1 + C(T-T_c)\, \delta n(x, y, z=z_0, t) \tag{1}$$

Here $z=z_0$ denotes the coordinate of the section. Since the refractive index fluctuations are proportional to the order-parameter fluctuations δM (here the concentration fluctuations), Eq. (1) becomes

$$i(x, y) = i_0 + \delta i(x, y, t) \tag{2}$$

with

$$\delta i(x, y, t) \propto \delta M(x, y, z=z_0, t) \tag{3}$$

where i_0 is the average intensity.

In terms of image analysis, the signal that is obtained is discrete and corresponds to the integration of Eq. (2) over a volume element v. This volume v corresponds roughly to 1 pixel in the image and is of the order of a few pixels (depth of field) in the direction z. Moreover, the video scanning time (τ) has to be taken into account, which leads to a time integration during the scanning period $\tau = 40$ ms. Therefore the useful signal at the pixel located at (x_i, y_i) is

$$\delta i(x_i, y_i, t) \propto \langle \overline{\delta M(x, y, z=z_0, t)} \rangle_{v, \tau = 40\,\mathrm{ms}} \tag{4}$$

where $\langle\ \rangle$ denotes a spatial average and $\overline{\ }$ a temporal average.
In the temperature range investigated, the minimum relaxation time is always larger than 40 ms, so that the time integration has no influence. Equation (4) can thus be rewritten as

$$\delta(x_i, y_i, t) \propto \langle \delta M(x, y, z=z_0), t \rangle_v \tag{5}$$

After having been detected by the camera, the image is stored on a videotape and later digitized with 64 levels (6 bits) and over 256×256 pixels. Typical images are shown in Fig. 2. A number of numerical treatments (accuracy 16 bits) are then performed.

The inhomogeneities of the incident beam and of the camera response, dusts on the windows, etc., are lowered by subtracting from the image under study another image taken at $T \gg T_c$, where fluctuations are no longer visible. Then a histogram of the intensity levels is calculated (Fig. 3), which allows the average intensity i_0 to be determined. More specific treatments are given below (see Section 3.2).

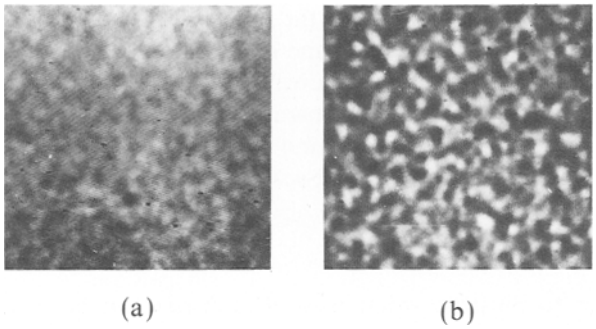

Fig. 2. Photographs of concentration fluctuations in the binary fluid of isobutyric acid and water. The field of view corresponds to 250 μm. (a) $T - T_c = 16$ mK; (b) $T - T_c = 1$ mK.

A number of binary fluids have been investigated: nitrobenzene–*n*-hexane, lutidine–water, isobutyric acid–water, lutidine–water, methanol–cyclohexane and its deuterated derivatives, and a microemulsion of dodecane–pentanol–water–sodium dodecyl sulfate (SDS). Fluctuations can be seen only in a range of concentration and temperature close to criticality: $|c - c_c| \simeq [0 - 0.03]$, $T - T_c(\text{mK}) \simeq [1 - 25]$. The bulk character of these fluctuations was clearly evidenced by changing the plane of focus and by stirring the system. The dynamics of such fluctuations is striking; they develop and vanish at a rate which is a function of their size and of temperature. If one selects a fluctuation wavelength ($/\backslash$) by allowing only the

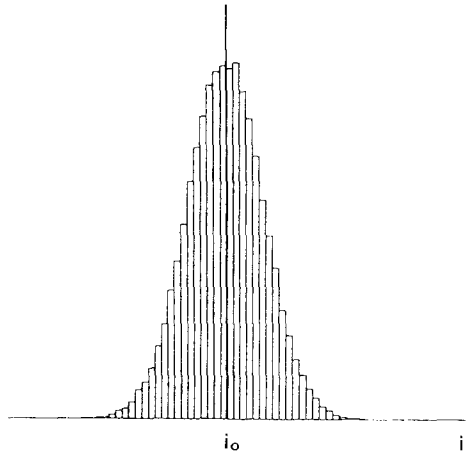

Fig. 3. Histogram of a picture taken at $T - T_c = 1$ mK (isobutyric acid–water mixture).

light scattered at $k = 2\pi/\Lambda$ to form the image (e.g., by putting a mask with an eccentric pinhole in the focal plane of the lens), the corresponding typical frequency goes to zero with decreasing k and decreasing $T - T_c$. This is in full agreement with critical dynamics [1]. We did not investigate this aspect further because the information that can be obtained seemed to be the same as that inferred from light-scattering techniques.

3. CRITICAL FLUCTUATIONS

In order to illustrate what new phenomena can be investigated, we report the preliminary study of two different problems.

3.1. Statistics of Fluctuations and Free Energy

On general grounds the intensity distribution function $P\{\delta i(x_i, y_i, t)\}$ of a given distribution $\{\delta i(x_i, y_i, t)\}$ at time $t = t_0$ (that we omit in the following since we deal only with statics) which corresponds to a partition function Z and a dimensionless free energy $F\{\delta i(x_i, y_j)\}$ is defined as

$$P\{\delta i(x_i, y_i)\} = \frac{1}{Z} \exp\left[-\sum_i F\{\delta i(x_i, y_i)\} \right] \tag{6}$$

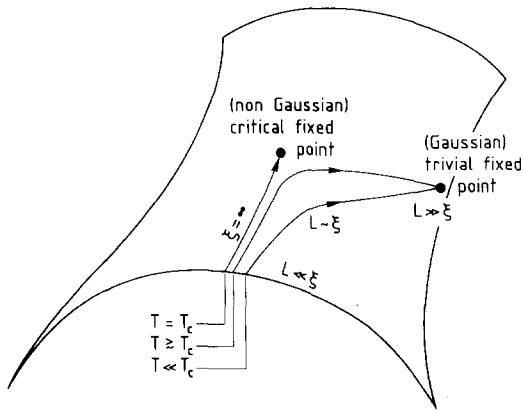

Fig. 4. Sketch of the renormalization trajectories. Starting at a scale $L \ll \xi$, the renormalization process continues up to a scale $L \gg \xi$. Here, when $T \neq T_c$ (ξ finite), all trajectories converge to the (trivial) fixed point, where the statistics of fluctuations is Gaussian. When $T = T_c$ ($\xi = \infty$), the trajectory goes to another fixed point (critical), where statistics are non Gaussian. Our study starts in an intermediate regime $L \gtrsim \xi$.

How is this experimental quantity related to the singular free energy of the real system near T_c? This question relates directly to the meaning of the renormalization trajectories in the renormalization-group theory (Fig. 4) [4]. Starting from a nonsingular free energy, a renormalization over volume L^3 leads to an energy singular in $T-T_c$ and a Gaussian statistic when $L \gg \xi$ (trivial fixed point), except for $T = T_c$. Our experiment, performed at a resolution $L \simeq 1$ pixel $\gtrsim \xi$, therefore corresponds to an intermediate state on the renormalization trajectory. A deviation compared to what is found at the fixed point can be reasonably expected.

The analysis of $P\{\delta i\}$, i.e., of the histogram (Fig. 3) shows that the probability distribution is Gaussian, with a temperature-dependent first moment

$$-\log P \sim F = (\varepsilon)(\delta i)^2$$

with $\varepsilon = (T/T_c) - 1$. A prediction which can be compared with the experimental situation has been made by Bervillier and Bagnuls [5]. The temperature ε gives a value for the ratio $[L/\xi(\varepsilon)]$ and therefore determines the location of the experiment on the renormalization trajectory (Fig. 4). By varying L at given ε, one can expect a measurement of the exponent ν by this "experimental" renormalization technique. That this exponent could be measured in the vicinity of T_c without varying the temperature is unusual but is a direct consequence of the renormalization-group theory.

Unfortunately a precise comparison with the experiment is complicated by a background (B) contribution which comes from the noise associated with the image subtraction (Fig. 5). We expect a more satisfac-

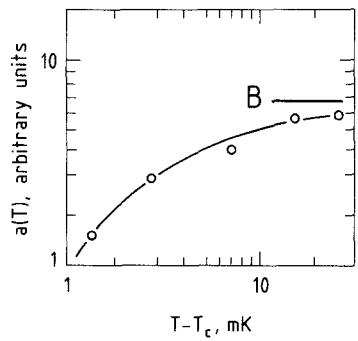

Fig. 5. Variation of the inverse width $a(T)$ of the histogram of intensity fluctuations (see text). B is a background contribution from the camera noise.

tory comparison with a new image analysis system that we are presently setting up. A significant improvement might also be performed by using ternary mixtures where the correlation length is longer. Finally, further experiments up to $T-T_c \simeq 0.1$ mK seem feasible without major difficulties, which might allow ratios $(L/\xi) \lesssim 0.1$ to be reached.

3.2. Morphology of Fluctuations

Fluctuations can be considered as clusters or domains. A precise definition of these domains is not unambiguous, however. The more obvious assumption is to call a domain the locus of connected pixels where intensity $i(x_i, y_i)$ exceeds an arbitrary value i_1:

$$i(x_i, y_i) > i_1 \tag{7}$$

This will separate the image into "white" clusters ($i \geqslant i_1$) and "black" clusters ($i < i_1$). The more natural choice is, of course, to make $i_1 = i_0$, the average value of the histogram of intensity levels (Fig. 3).

Such domains are reported in Fig. 6. They clearly do not resemble compact clusters. In order to determine to what extent they might be fractal objects, we calculated for each domain (p), characterized by its center of mass (x_p, y_p), its mass

$$m_p = \sum_{i \in p} 1 = n \text{ pixels} \tag{8}$$

and its gyration radius

$$R_p = \left[\frac{1}{m_p} \sum_{i \in p} (x_i - x_p)^2 + (y_i - y_p)^2 \right]^{1/2} \tag{9}$$

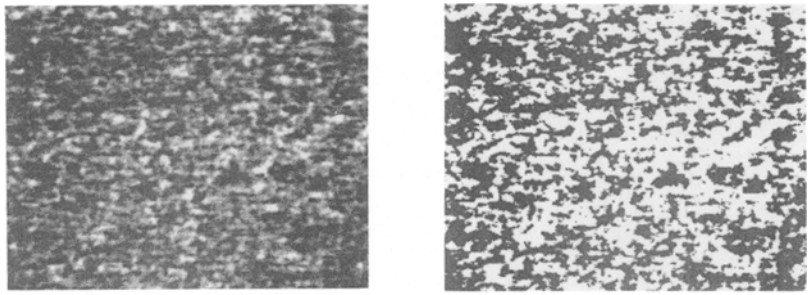

Fig. 6. Fluctuation pattern before (a) and after (b) digitization at two levels ($T - T_c = 1$ mK). (Same scale as in Fig. 2).

The variation of m_p with respect to R_p is reported in Fig. 7. The fact that over more than three decades a linear relationship is obtained between $\log R_p$ and $\log m_p$ demonstrates self-similarity. The associated fractal exponent d_f, defined by

$$m_p \sim R_p^{d_f} \tag{10}$$

has been found to be (case $i_1 = i_0$)

$$d_f = 1.8 \pm 0.1$$

In the above determination of d_f, small clusters (smaller than 5 μm) have been ignored. The final error accounts for the known sources of uncertainties and is much larger than the statistical deviation. This value did not vary systematically with temperature. Changing the threshold (i_1) moves d_f to

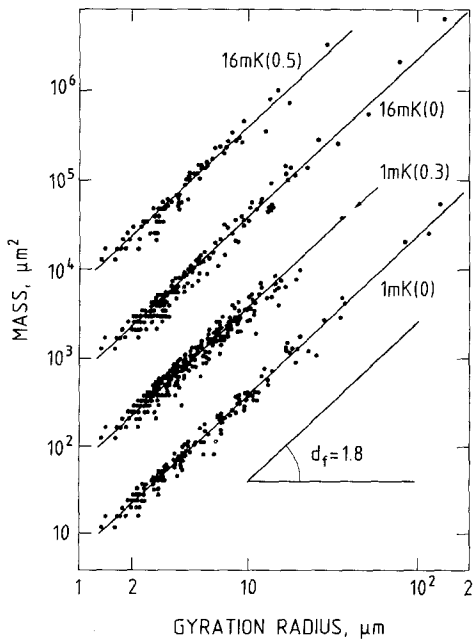

Fig. 7. Self-similarity of fluctuation clusters: mass of clusters with respect to their gyration radius. Typical data at two temperatures are reported, with typical intensity thresholds in parentheses. These are expressed as deviations from the average intensity in units of the fluctuation histogram full-width. Because all data overlap, they have been shifted by one decade for clarity.

1.7 and lowers the range of available gyration radius. Since the value found is not very far from 2, which is the dimension of compact clusters, we checked all the procedures of measurement by taking the image of an assembly of dense circular dots of various dimensions. The same analysis as before gave $d_f = 2.00 \pm 0.02$.

The domains that have been analyzed are in fact the planar sections of 3-D domains. The relationship between a 3-D fractal object and a 2-D section has been evocated by Mandelbrot [6]; the fractal dimension of the section (d_f) is related to the fractal dimension D_f of the 3-D object through

$$D_f = 1 + d_f \tag{11}$$

This relationship is obvious for dense domains. The fractal dimension of the 2-D projection of a 3-D object has been studied by Tence *et al.* [7]. When the thickness of the projection tends to zero, one recovers the above result. The fractal dimension of the critical fluctuations according to Eq. (11) is therefore

$$D_f = d_f + 1 = 2.8 \pm 0.1$$

That such fluctuations are fractal objects might appear to be very surprising. But this is not really so, as we explain in the following.

Fractal fluctuations can indeed be obtained with an "ad hoc" definition for the clusters. The basic idea relies on the fact that critical fluctuations diverge at T_c. The percolation correlation length (ξ_p) eventually associated with the fluctuating domains should diverge also. In order that the percolation correlation length and the thermal correlation length diverge at the same (critical) temperature, with the same exponents, a special (and rather artificial) definition of the critical clusters (the so-called "physical clusters") had to be made [8]. Then the fractal nature of such clusters comes naturally from the percolation character of the transition. Their fractal dimensionality is expected to be

$$D_f = D - \beta/\nu \simeq 2.5$$

Here $D = 3$ and the values $\beta = 0.325$ and $\nu = 0.630$ are those of the 3-D Ising model. This value is different from our finding $D_f = 2.8$.

Note that the existence of fractal fluctuations is not in disagreement with the form of the structure factor at large k,

$$S(k) \sim k^{-(2-\eta)} \tag{12}$$

with $\eta \simeq 0.03$ the universal Fisher exponent. For monodisperse fractals

$$S(k) \sim k^{-D_f} \tag{13}$$

so that a naive reasoning would give $D_f \simeq 1.97$. However, the distribution of mass of clusters $P(m)$ modifies this result. With τ the associated exponent

$$P(m) \sim m^{-\tau} \tag{14}$$

the structure factor at large k [9] is

$$S(k) \sim k^{-D_f(3-\tau)} \tag{15}$$

The comparison with Eq. (12) gives

$$D_f = \frac{2-\eta}{3-\tau} \simeq 2.5 \tag{16}$$

when using the value $\tau \simeq 2.2$, which is generally found in the 3-D percolation problems [10].

However, the above arguments are based on the behavior of the correlation function of the fluctuations at short distance $r < \xi$, where the correlation function of fluctuations can be estimated as

$$\langle \delta M(0)\, \delta M(r) \rangle \sim r^{-(1+\eta)} \tag{17}$$

In contrast, our study was performed in the range $r \gtrsim \xi$.

The fractal character of clusters at this scale might also be due to a correlated percolation of sites (pixels) in the observed picture. Such a percolation mechanism leads indeed to the formation of domaïns in two dimensions with the fractal dimensionality [11]

$$d_f \simeq 1.9$$

This last value is not very different from our experimental finding of $d_f = 1.8$

4. CONCLUSION

In this paper we have tried to convince the reader that the direct visual observation of critical fluctuations makes it possible to investigate new and exciting problems, including the study of the fluctuations statistics at different length scales and the connection of thermal critical points to percolation critical points.

ACKNOWLEDGMENTS

We have benefited from fruitful discussions with E. Brézin, H. Herrmann, C. Bagnuls, and C. Bervillier and also with M. E. Fisher during this conference.

REFERENCES

1. See, e.g., *Phase Transitions*, M. Levy, J. C. Le Guillou, and J. Zinn-Justin, eds. (Plenum, New York, 1982).
2. P. Debye and R. T. Jacobsen, *J. Chem. Phys.* **48**:203 (1968).
3. R. Plazza, T. Bellini, V. Degiorgio, R. E. Goldstein, S. Leibler and R. Lipowsky, *Phys. Rev. B* **38**:7223 (1988).
4. See, e.g., K. G. Wilson, *Sci. Am.* **241-2**:140 (1979); K. G. Wilson and J. Kogut, *Phys. Rep.* **12C**:75 (1974).
5. C. Bervillier and C. Bagnuls, Private communication (1988).
6. See, e.g., B. B. Mandelbrot, *The Fractal Geometry of Nature* (Freeman, San Francisco, 1982).
7. M. Tence, J. P. Chevalier, and R. Jullien, *J. Phys.* **47**:1989 (1986).
8. See, e.g., S. Hayward, D. Heermann, and K. Binder, *J. Stat. Phys.* **49**:1053 (1987).
9. See, e.g., J. Teixeira, in *On Growth and Form*, H. E. Stanley and N. Ostrowsky, eds. (Nijhoff, Boston, 1986).
10. See, e.g., A. Aharony, in *Directions in Condensed Matter Physics, Memorial Volume in Honor of Sheng-Keng Ma*, G. Grinstein and G. Mazenko, ed. (Singapore World Scientific, 1986).
11. F. Family, in *Universalities in Condensed Matter*, R. Jullien, L. Peliti, R. Rammal, and N. Boccara, eds. (Springer, Heidelberg, 1988).